Inorganic Chemistry

Article

pubs.acs.org/IC

New Quaternary Chalcogenides, $Tl_{18}Pb_2M_7Q_{25}$ (M = Ti, Zr, and Hf; Q = S and Se): Crystal Structure, Electronic Structure, and Electrical Transport Properties

Cheriyedath Raj Sankar, Anna Becker, Abdeljalil Assoud, and Holger Kleinke*

Department of Chemistry and Waterloo Institute for Nanotechnology, University of Waterloo, Waterloo, Ontario, Canada N2L 3G1

Supporting Information

ABSTRACT: We have synthesized new quaternary chalcogenides of the general formula $Tl_{18}Pb_2M_7Q_{25}$ (M = Ti, Zr and Hf, Q = S, Se), and studied their crystal and electronic structures. They are all isostructural, with a large cubic unit cell of space group $Pa\bar{3}$, and a = 17.0952(6) Å in case of $Tl_{18}Pb_2Ti_7S_{25}$ (with four formula units per cell). The structure is composed of several interesting subunits such as isolated M_7Q_{24} entities, weakly connected Tl_9Pb supertetrahedra (or 4-capped distorted octahedra) and STl_6 distorted octahedra. The finite unit M_7Q_{24} is formed by seven edge-shared MQ_6 octahedra wherein all except the central one are distorted because of the neighborhood of Tl^+ ions that carry a lone pair of electrons. These materials are semiconductors with all elements in their common oxidation states, for example, $(Tl^+)_{18}(Pb^{2+})_2(Ti^{4+})_7(S^{2-})_{25}$. The calculations yielded band gaps of 0.64 eV for the sulfides $Tl_{18}Pb_2Ti_7S_{25}$ and 1.0 eV for $Tl_{18}Pb_2Zr_7S_{25}$. The selenide $Tl_{18}Pb_2Ti_7Se_{25}$ was calculated to have a band gap of 0.44 eV. Electrical conductivity measurements and reflectance spectroscopy also revealed the semiconducting nature of these samples, with experimentally determined gaps between 0.10 and 0.50 eV.

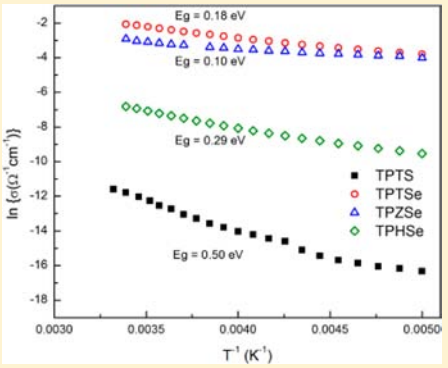

INTRODUCTION

Heavy-metal chalcogenide narrow-gap semiconductors are important materials for various applications such as thermoelectric[1−4] and detector materials.[5−8] Several thallium containing ternary and quaternary chalcogenides[4−7] offer great promise toward these applications. A few layered compounds, namely, $TlSbTe_2$,[9] $TlBiTe_2$,[10] and $TlGdTe_2$[11] have been found interesting because of their thermoelectric properties, mostly caused by the low lattice thermal conductivity. Besides the large weight of Tl, which is advantageous for forming compounds of low thermal conductivity, the presence of a lone pair of electrons of monovalent Tl ions results in distorted coordination environments. This in turn results in complex structures, for example, as in Tl_9BiTe_6, a promising thermoelectric.[4] Recently, it was reported that the lone pair of electrons in certain ternary chalcogenide systems has a significant effect on lattice thermal conductivity by creating anharmonicity in the lattice.[12] With these viewpoints, Tl-based thermoelectrics require further attention and demand more exploration.

During our recent research in the area of ternary thallium chalcogenides with group 4 elements, we have uncovered and characterized several new compounds, such as Tl_2MQ_3[13,14] and Tl_4MQ_4[15,16] where, M = Zr, Hf and Q = S, Se, and Te. Of these, the tellurides form different structures compared to those of the selenides and sulfides. Tl_2ZrTe_3 is unique in the Tl_2MQ_3 family, which adopts a cubic structure with a large unit cell (a = 19.118 Å).[14] Tl_2ZrTe_3 is a narrow band gap semiconductor; however, it decomposes in an open system around 450 K, making it unusable for high-temperature applications. Tl_2MS_3 and Tl_2MSe_3 belong to another structure type (monoclinic, $P2_1/m$), forming a layered structure, but they are large band gap semiconductors and thus highly resistive in nature.[13] The other class, Tl_4MQ_4, also has two different structure types; the tellurides crystallize in a trigonal lattice while the sulfides and selenides form a triclinic structure. Tl_4MTe_4 contains $ZrTe_6$ octahedra that are face-condensed to form unique isolated, trimeric chains in the lattice.[16] Zr and Hf form such tellurides while the corresponding Ti compound was not obtained. The sulfides and selenides are composed of edge-shared ZrQ_6 octahedra that form a zigzag chains.[15] All of these compounds contain weak, yet significant, Tl−Tl interactions.

Other related compounds are the ones of the type A_2MQ_3, where A is an alkali metal ion, like Na, K, or Rb.[17,18] Even though Tl^+ resembles A^+ in its size and monovalent nature, the crystal structure and bonding properties are quite different in these ternary compounds owing to the difference in electronegativity and the stereochemical activity of the $6s^2$ electrons of Tl^+. Monovalent Cu ions also form similar type of compounds as in the cases of Cu_2MTe_3 (space group $C2/m$)[19,20] and $TlCuMQ_3$ (space group $Cmcm$).[21] There are several other Tl-M'-Q compounds where M' is a tetravalent group 14 ion.[22−27] Our recent attempts to explore more heavy metal chalcogenides in the related series of compounds led us to discover a new class of compounds, namely, $Tl_{18}Pb_2M_7Q_{25}$. In this paper

Received: September 25, 2012
Published: February 1, 2013

   dx.doi.org/10.1021/ic3020699 | Inorg. Chem. 2013, 52, 1895−1900

Table 1. Crystallographic Information of the Five Compounds Obtained from Single Crystal X-ray Diffraction Studies

refined formula	$Tl_{18}Pb_2Ti_7S_{25}$	$Tl_{18}Pb_2Ti_7Se_{25}$	$Tl_{18}Pb_2Zr_7S_{25}$	$Tl_{18}Pb_2Hf_7S_{25}$	$Tl_{18}Pb_2Hf_7Se_{25}$
formula weight [g/mol]	5229.84	6402.34	5533.08	6143.97	7316.47
T of measurement [K]	296(2)	296(2)	296(2)	296(2)	296(2)
wavelength [Å]	0.71073	0.71073	0.71073	0.71073	0.71073
crystal system	cubic	cubic	cubic	cubic	cubic
space group	$Pa\bar{3}$	$Pa\bar{3}$	$Pa\bar{3}$	$Pa\bar{3}$	$Pa\bar{3}$
a [Å]	17.0952(6)	17.676(2)	17.463(3)	17.4489(8)	18.001(3)
V [Å^3]	4996.0(3)	5522.5(9)	5325.3(1)	5312.6(4)	5833(2)
Z	4	4	4	4	4
ρ_{calcd} [g/cm^3]	6.953	7.7	6.901	7.682	8.331
$R1/wR2$ $(I > 2\sigma(I))^a$	0.0522/0.0646	0.0999/0.1304	0.1025/0.1376	0.0527/0.0814	0.0603/0.0737

$^a R1 = \sum||F_o| - |F_c||/\sum|F_o|$; $wR2 = [\sum w(F_o^2 - F_c^2)^2/\sum w(F_o^2)^2]^{1/2}$.

Table 2. Atomic Positions of $Tl_{18}Pb_2Ti_7S_{25}$

atom	Wyckoff site	x	y	z	U_{eq} / Å^2
Tl1	24d	0.31850(3)	0.48338(3)	0.32464(3)	0.0251(1)
Tl2	24d	0.16889(3)	0.32020(3)	0.34230(3)	0.0256(1)
Tl3	24d	0.17160(3)	0.47983(3)	0.48588(3)	0.0240(1)
Pb1	8c	0.18203(2)	0.18203(2)	0.18203(2)	0.0211(2)
Ti1	24d	0.0121(1)	0.15708(10)	0.3504(1)	0.014(3)
Ti2	4b	$^1/_2$	$^1/_2$	$^1/_2$	0.018(1)
S1	24d	0.0058(2)	0.2952(1)	0.3558(2)	0.0171(5)
S2	24d	0.0083(1)	0.1432(1)	0.4989(1)	0.0108(4)
S3	24d	0.02100(1)	0.1524(1)	0.2114(1)	0.0158(5)
S4	24d	0.1466(1)	0.3663(1)	0.1524(1)	0.0135(4)
S5	4a	0	0	0	0.054(3)

we describe the synthesis and electrical transport properties of these materials.

EXPERIMENTAL SECTION

Syntheses and Phase Purity Analyses. The first sample obtained was $Tl_{18}Pb_2Ti_7S_{25}$ during our attempts to synthesize a quaternary material of the same elements, and the chemical formula was obtained from a single crystal X-ray diffraction analysis. Subsequently, the whole series of compounds were synthesized from the respective elements stored in an argon-filled glovebox (Tl granules, 99.9% (Alfa Aesar); Ti powder −150 mesh, 99.9% (Alfa Aesar); Zr pieces, ≈2 mm, 99.5% (Alfa Aesar); Hf powder −100 mesh, 99.6% (Alfa Aesar); S flakes, 99.99% (Aldrich), and Se pellets, ≈2−3 mm, 99.99% (Aldrich). The required stoichiometric amounts of the individual elements were weighed into quartz ampules and sealed under vacuum. The ampules were heated slowly to 1073 K in a resistance furnace, allowed to remain at 1073 K for 100 h, and finally slowly cooled down to 723 K at which point the furnace was switched off to allow for cooling to room temperature. The products were analyzed by using powder X-ray diffraction experiments of the samples performed on an Inel powder diffractometer (XRG3000) with position-sensitive detector and Cu-$K\alpha_1$ radiation. Our attempts to synthesize the corresponding tellurides, however, were not successful at various reaction conditions, yielding Tl_5Te_3-type product predominantly, as evidenced from the corresponding powder X-ray patterns. We were also not able to synthesize any corresponding Sn (substituted for Pb or Ti) and Ge (substituted for Ti) analogues.

Single-Crystal Structure Determinations. Suitable single-crystals (blocks) were picked from the respective bulk sample and mounted on glass fibers using epoxy glue for the single-crystal X-ray diffraction (XRD) analysis. The data were collected at room temperature, by using a Bruker Smart Apex CCD diffractometer that employs Mo-$K\alpha$ radiation, by scans of 0.3° in ω at two different φ angles with exposure times of 30 s each for a total of minimum two blocks of 600 frames each. The data were treated for Lorentz and polarization corrections. The absorption corrections were based on fitting a function to the empirical transmission surface as sampled by multiple equivalent measurements using SADABS included in the package SAINT[28] within APEX2 software.[29]

The structures of five compounds in the whole series were solved and refined in the cubic space group $Pa\bar{3}$. No suitable single crystals for the single crystal XRD measurement were obtained for the sample $Tl_{18}Pb_2Zr_7Se_{25}$; however, the powder XRD pattern of the sample showed that it is isostructural with the other five described in this study. The SHELXTL program was used for the structure refinement.[30] The first compound to be discovered in this class was the one with the formula $Tl_{18}Pb_2Ti_7S_{25}$. Here, the unit cell consists of four such formula units. The final R1 and wR2 values ($I > 2\sigma$) were found to be 0.052 and 0.065, respectively. The high values of the anisotropic displacement parameters of atom S5 in all sulfides were not consistent with those of Se5 of selenides, and hence no split positions were considered during the refinement. Finally, the program TIDY included in the PLATON package[31] was used to obtain the standardized atomic positions. The crystallographic details of all five compounds are given in Table 1, and the atomic positions and equivalent displacement parameters of $Tl_{18}Pb_2Ti_7S_{25}$ in Table 2.

Electronic Structure Calculations. For the first-principles calculation of the electronic structure, we used the WIEN2k code, which employs the full-potential linearized augmented plane wave (FP-LAPW) method within Kohn−Sham density functional theory (DFT).[32] The generalized gradient approximation (GGA) from Perdew, Burke, and Ernzerhof (PBE) was used for exchange and correlation energies.[33,34] We used the following muffin-tin radii (R_{MT}): 2.5 Bohr for Tl and Pb, 2.36 for Ti in $Tl_{18}Pb_2Ti_7S_{25}$ and 2.49 for Ti in $Tl_{18}Pb_2Ti_7Se_{25}$, 2.40 for Zr, 2.09 for S in $Tl_{18}Pb_2Ti_7S_{25}$ and 2.13 for S in $Tl_{18}Pb_2Zr_7S_{25}$, 2.21 for Se. The product $R_{MT} \times K_{Max}$ was set to be 7. For the self-consistent energy calculations, 11 k points were selected (out of 200) with an improved tetrahedron method within the irreducible wedge of the first Brillouin zone. The charge and energy convergence were set to of 10^{-4} for the self-consistency calculation. The total density of states (DOS) were calculated as well as the atomic contributions. Reduction of Gauss broadening parameter from 0.003 to 0.001 yielded a perfect edge at the Fermi level (and hence band gaps) in DOS curves compared to the smoothened DOS curves, and

dx.doi.org/10.1021/ic3020699 | Inorg. Chem. 2013, 52, 1895−1900

the former is used for band gap determination. The large unit cell with 208 atoms in it restricted our calculations, and thus the band structures are not determined. For the same reason, we could not perform the calculations with the spin−orbit interactions included.

Physical Property Measurements. The samples were ground well and pressed into rectangular pellets of the approximate dimensions 13 × 2 × 2 mm by applying a pressure of 770 MPa. The electrical transport measurements were carried out on a home-assembled set up that employs a four probe method. The samples were attached to silver wires with the aid of silver paste. A Keithley model 2400 source/measure unit was used to pass a constant current through the sample and measure the corresponding voltage at various temperatures below the room temperature. The sample was cooled with the aid of a closed cycle Helium refrigerator. The room temperature resistivity values of $Tl_{18}Pb_2Zr_7S_{25}$ and $Tl_{18}Pb_2Hf_7S_{25}$ were found to be too large and consequently, low-temperature measurements were not carried out. Tentative measurements of the Seebeck coefficient of $Tl_{18}Pb_2Ti_7Se_{25}$ and $Tl_{18}Pb_2Zr_7Se_{25}$ were performed between 300 and 500 K using the ULVAC-RIKO ZEM-3 under helium atmosphere as described before.[35,36]

Finally, an optical band gap measurement was performed for $Tl_{18}Pb_2Ti_7S_{25}$ using the Bruker Vertex 70 FT-IR spectrometer in diffuse reflectance mode under ambient conditions.

RESULTS AND DISCUSSION

Crystal Structures. Group 4 elements, namely, Ti, Zr, and Hf, form $Tl_{18}Pb_2M_7Q_{25}$ type of sulfides and selenides which all crystallize in the cubic space group $Pa\bar{3}$. The unit cell length increases from the sulfides to selenides as evidenced from $Tl_{18}Pb_2Ti_7Q_{25}$ (a = 17.10 Å and 17.68 Å for sulfide and selenide) and $Tl_{18}Pb_2Hf_7Q_{25}$ (17.45 Å and 18.0 Å for sulfide and selenide) compounds. Among the sulfides, the unit cell parameter a is the largest for the Zr sulfide (17.46 Å), which is significantly larger than the Ti sulfide and only slightly larger than the Hf sulfide. This is expected according to the respective atomic radii of the elements. The structural features are discussed below for $Tl_{18}Pb_2Ti_7S_{25}$, whose unit cell is shown in the left part of Figure 1, wherein the Ti−S polyhedra are emphasized.

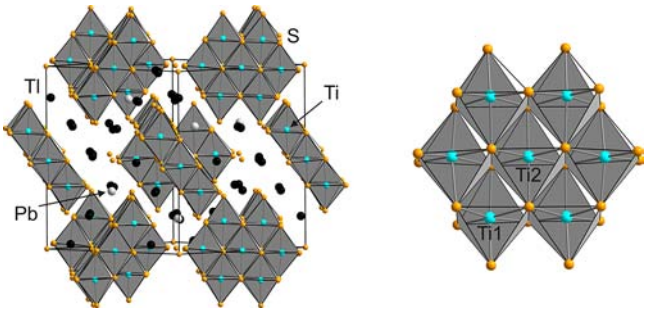

Figure 1. Crystal structure of $Tl_{18}Pb_2Ti_7S_{25}$ (left) and its $[Ti_7S_{24}]^{20-}$ unit (right).

The two crystallographically distinct Ti atoms are both surrounded by six S atoms in the form of distorted octahedra. The TiS_6 octahedra share corners and edges to form $[Ti_7S_{24}]^{20-}$ motifs with all Ti atoms of this unit approximately lying in the same plane, while the $[Ti_7S_{24}]^{20-}$ motifs are separated from one another by intervening Tl and Pb atoms. The $Ti2S2_6$ octahedron builds the center of this $[Ti_7S_{24}]^{20-}$ unit, and is only slightly distorted with S−Ti−S angles of 86°, in contrast to the larger distortion of the other TiS_6 "octahedron". This fragment is shown in the right part of Figure 1. Herein, Ti−S distances range from 2.36 Å to 2.55 Å, with the one Ti2−S2 distance being 2.45 Å, while the corresponding Ti−S distance in TiS_2 (CdI_2 type) is 2.42 Å.[37]

There are five crystallographically distinct S atoms and except for S5, all others are connected to Ti atoms. The S5 atom is only bonded to Tl atoms like in the earlier discovered Tl_2ZrTe_3,[14] wherein one of the Te sites is only connected to Tl atoms, a feature also similar to Ba coordinated Se/Te sites in $Ba_7Sn_3Se_{13}$[38] and $NaBa_6Cu_3Te_{14}$.[39]

Though we have assigned distinct sites for Tl and Pb, an argument that Tl and Pb can be mixed occupied cannot be completely ruled out, for their space requirements and the scattering power of X-rays are comparable. Our assignment is based on the general picture obtained from the nature of Tl−S and Pb−S bonds in various compounds, which suggest that Pb prefers to be in more symmetric and hexa-coordinated (or higher) coordination when compared to mostly unsymmetrical coordination of Tl with fewer chalcogen atoms. For instance, Tl_2S (deformed anti-CdI_2-type)[40] and PbS (NaCl-type)[41] may be taken as typical examples within binaries, wherein Tl is connected to three S atoms, while Pb has a perfect octahedral arrangement of S around it. Though a stereochemical activity can be expected in both Tl^+ and Pb^{2+} due to $6s^2$ lone pairs, the greater charge on Pb^{2+} might require more anions around it, when compared to Tl^+ ion. Thus, Pb is distinguished from Tl1 and Tl2 in the structure of $Tl_{18}Pb_2Ti_7S_{25}$, which are surrounded by only five S atoms at distances ranging from 2.84 to 3.34 Å (Table 3), the distances and coordination being quite similar to those of Tl_4ZrS_4.[15] Within the hexa-coordination of Pb and Tl by S atoms, Pb would be expected to form shorter Pb−S bonds than Tl−S bonds. In Tl_2ZrS_3[13] and $PbZrS_3$,[42] the Tl and Pb atoms are six-coordinated by S atoms, both irregularly octahedral, but the Pb−S distances (2× 2.73 Å, 2.87 Å, 3.05 Å, and 2× 3.38 Å, average of 3.02 Å) are shorter than the Tl−S

Table 3. Selected Metal−S Distances of $Tl_{18}Pb_2Ti_7S_{25}$

atom 1	atom 2	count	distance (Å)
Tl1	S1		3.046(3)
	S2		3.197(3)
	S2		3.222(3)
	S3		3.057(3)
	S4		2.922(2)
Tl2	S1		2.830(3)
	S1		3.300(3)
	S3		3.115(3)
	S4		3.010(2)
	S4		3.362(2)
Tl3	S1		2.886(3)
	S1		3.322(3)
	S2		3.210(3)
	S3		2.927(3)
	S3		3.340(3)
	S5		2.9635(4)
Pb1	S3	3×	2.844(2)
	S4	3×	3.247(3)
Ti1	S1		2.366(3)
	S2		2.551(3)
	S2		2.555(3)
	S3		2.382(3)
	S4		2.421(3)
	S4		2.495(3)
Ti2	S2	6×	2.451(2)

dx.doi.org/10.1021/ic3020699 | Inorg. Chem. 2013, 52, 1895−1900

ones (2× 2.99 Å, 3.14 Å, 3.21 Å, and 2× 3.39 Å, average of 3.19 Å). In the present structure, the Tl3 and Pb1 sites are both 6-fold coordinated, with distances to S atoms from 2.84 Å to 3.34 Å. In both $Tl_{18}Pb_2Ti_7S_{25}$ and $Tl_{18}Pb_2Zr_7S_{25}$, the Tl3−S average distances (3.11 Å and 3.13 Å) are shorter than the respective Pb1−S distances (3.01 Å and 3.07 Å), and the TlS_6 polyhedron less regular. Finally, the slow cooling is also in support with an ordered structure, and the multiplicities of these sites (24 for Tl1, Tl2, Tl3, 8 for Pb1) are in agreement with the formula $Tl_{18}Pb_2Ti_7S_{25}$ as obtained from the phase pure syntheses, which matches the expectations of the common oxidation states according to $(Tl^+)_{18}(Pb^{2+})_2(Ti^{4+})_7(S^{2-})_{25}$.

Bond-valence sum calculations may also be used to verify the validity of our assignments of the Tl and Pb sites. The bond valences, v_{ij}, are calculated via $v_{ij} = \exp[(R_{ij} - d_{ij})/0.37\ Å]$ according to Brese and O'Keeffe.[43] Therein, d_{ij} is the distance between the two atoms i and j, and R_{ij} was empirically derived from the literature. To see which of the Tl/Pb sites would have the largest valence, and thus be the most likely to be chosen by Pb, we used the Tl−S distance of 2.63 Å for all these four sites. The resulting bond valence sums are then 1.51−1.86 for Tl1 to Tl3, compared to 2.25 for Pb1.

Several distances between the metal atoms Tl and Pb point to significant (weak) interactions, for example, those in the range of 3.59 to 3.97 Å may be considered as weak interactions. Homonuclear Tl−Tl interactions occur in many Tl-containing binary and ternary chalcogenides such as in Tl_5Te_3,[44,45] TlTe,[46] Tl_4ZrTe_4,[16] and Tl_4ZrS_4.[15] For instance, Tl_4ZrTe_4 contains several Tl−Tl distances ranging from 3.49 Å to 4.03 Å, which all were found to be significantly bonding from the electronic structure calculations, by comparing their integrated crystal orbital Hamilton population (ICOHP) values with those of elemental hexagonal modification of Tl (where the shortest Tl−Tl distance is 3.40 Å).

The weak Tl/Pb−Tl/Pb interactions in $Tl_{18}Pb_2Ti_7S_{25}$ yield a Tl_9Pb supertetrahedral cluster, which may be depicted as a distorted Tl_6 octahedron with three capping Tl and one Pb atoms (Figure 2). This supertetrahedron forms the metal core

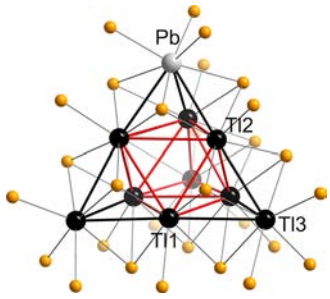

Figure 2. Tl_9Pb supertetrahedron of $Tl_{18}Pb_2Ti_7S_{25}$ including its surrounding S atoms.

of the Tl_9PbS_{54} unit. Herein, the metal atom at each corner is connected to six S atoms and those lying at the edges are connected to five S atoms. Within the structure of $Tl_{18}Pb_2Ti_7S_{25}$, these giant supertetrahedra are decorated around the unique STl_6 unit, each Tl atom of which renders a corner for the former. The Ti_7S_{24} units are enclosed by eight such supertetrahedral units.

A supertetrahedral framework is usually reminiscent of the P_4O_{10} molecular structure, which is of adamantane-type. In this case, the Tl and Pb positions are topologically equivalent to the O positions of P_4O_{10}. Supertetrahedra made from SiO_4 like entities are common in cristobalite frameworks and have been identified in several inorganic−organic hybrid compounds.[47−53] This Tl_9Pb cluster is also different from Tl-clusters found in metal thallides[54−58] and more recently discovered Cs_8Tl_8O,[59] $Rb_{10}Tl_6O_2$,[60] and Cs_4Tl_2O[61] thallide-oxides, with respect to the presence of strong Tl−Tl bonding interactions in the latter two classes of compounds.

Electronic Structures and Electrical Transport Properties. The absence of any homonuclear interaction <3.5 Å bodes well for the adoption of the common oxidation states of Tl^+, Pb^{2+}, $(Ti/Zr/Hf)^{4+}$, and $(S/Se)^{2-}$. Thus, these chalcogenides are likely semiconductors, as all atoms may be viewed as being closed-shells, according to, for example, $(Tl^+)_{18}(Pb^{2+})_2(Ti^{4+})_7(S^{2-})_{25}$. The calculated DOS curves of the representatives $Tl_{18}Pb_2Ti_7S_{25}$ and $Tl_{18}Pb_2Zr_7S_{25}$ confirm this, revealing band gaps of 0.64 and 1.0 eV, respectively (Figure 3). The valence band has predominant contributions

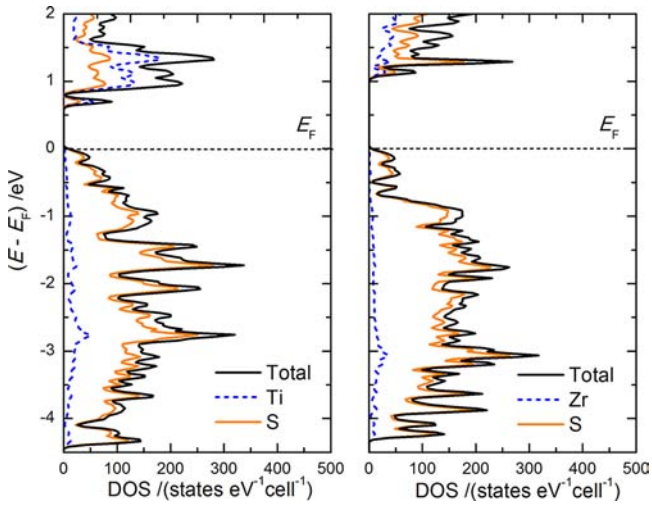

Figure 3. Density of states of $Tl_{18}Pb_2Ti_7S_{25}$ (left) and $Tl_{18}Pb_2Zr_7S_{25}$ (right).

from the 3p orbitals of S, whereas transition metal d orbitals, either from Ti or Zr, dominate in the conduction band. Tl and Pb orbitals are treated together and found to be insignificant near the Fermi level.

The selenide $Tl_{18}Pb_2Ti_7Se_{25}$ has a calculated band gap of 0.44 eV, wherein the valence band is predominantly composed of the 4p states of Se. The DOS for this compound is available as Supporting Information. (In all these plots, the DOS above E_F is nonzero because of the "smoothing" of the DOS curves. For the band gap calculation as we reported here, we ran the DOS calculation with little "smoothing".) Thus, a decrease of the calculated band gap from 0.64 to 0.44 eV was observed when we moved from the sulfide to the selenide. Similarly, the heavier group 4 element causes an increase of the band gap as calculated for $Tl_{18}Pb_2Ti_7S_{25}$ (0.64 eV) and $Tl_{18}Pb_2Zr_7S_{25}$ (1.0 eV). These trends can readily be understood based on electronegativity differences, because a more electronegative anion (S compared to Se) causes a lower lying valence band, and a more electronegative cation (Zr vs Ti) a higher lying conduction band, and thus a larger gap between valence and conduction band. It should be noted that the electronic structures obtained from calculation including spin−orbit coupling would most likely exhibit smaller band gaps. This

dx.doi.org/10.1021/ic3020699 | Inorg. Chem. 2013, 52, 1895−1900

was for example demonstrated for Tl_9SbTe_6, where the spin−orbit calculations yielded a gap of 0.37 eV, compared to 0.54 eV without spin−orbit.[62] Similarly, the band gap of $CsBi_4Te_6$ was calculated to be 0.04 eV with spin−orbit correction and 0.37 eV without (all performed using the PBE-GGA like in this work).[63,64] However, as these DFT calculations typically result in underestimated band gaps, the experimentally determined ones (e.g., 0.5 eV in case of Tl_9SbTe_6 and 0.1 eV in case of $CsBi_4Te_6$) may lie between the values obtained with and without the spin−orbit correction.

These trends are further supported by our conductivity measurements at room temperature, which revealed values of the order of 10^{-5} Ω^{-1} cm^{-1} for $Tl_{18}Pb_2Ti_7S_{25}$ and 10^{-8} Ω^{-1} cm^{-1} for both $Tl_{18}Pb_2Zr_7S_{25}$ and $Tl_{18}Pb_2Hf_7S_{25}$. The room temperature conductivity values of 1.1×10^{-1} Ω^{-1} cm^{-1}, 4.8×10^{-2} Ω^{-1} cm^{-1}, and 9.8×10^{-4} Ω^{-1} cm^{-1} were measured for the respective selenides, namely, $Tl_{18}Pb_2Ti_7Se_{25}$, $Tl_{18}Pb_2Zr_7Se_{25}$, and $Tl_{18}Pb_2Hf_7Se_{25}$. All the samples investigated here exhibit semiconducting behavior, namely, conductivity being exponentially decreased with decreasing temperature. Because of the very low conductivity of $Tl_{18}Pb_2Zr_7S_{25}$ and $Tl_{18}Pb_2Hf_7S_{25}$, no temperature dependence was measured, for lowering the temperature would yield too low (unmeasurable) conductivity values.

The logarithmic conductivity varies linearly when plotted against the inverse of temperature, which is shown in Figure 4

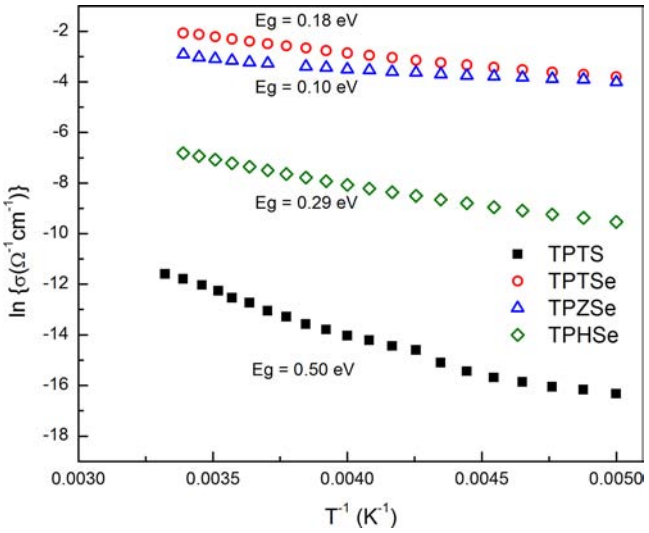

Figure 4. Electrical conductivity of $Tl_{18}Pb_2Ti_7S_{25}$ (TPTS), $Tl_{18}Pb_2Ti_7Se_{25}$ (TPTSe), $Tl_{18}Pb_2Zr_7Se_{25}$ (TPZSe), and $Tl_{18}Pb_2Hf_7Se_{25}$ (TPHSe).

for the temperature range of ∼150 K−300 K. The band gaps determined from this Arrhenius-type activation are 0.50 eV, 0.18 eV, 0.10 eV, and 0.29 eV for $Tl_{18}Pb_2Ti_7S_{25}$, $Tl_{18}Pb_2Ti_7Se_{25}$, $Tl_{18}Pb_2Zr_7Se_{25}$, and $Tl_{18}Pb_2Hf_7Se_{25}$, respectively. The optical band gap of $Tl_{18}Pb_2Ti_7S_{25}$ of 0.5 eV, as determined via diffuse reflectance spectroscopy (available as Supporting Information), confirms the size of the gap determined from the conductivity measurement, which is typical for undoped semiconductors. These two experimentally determined values of both 0.5 eV are slightly smaller than the computed gap of 0.64 eV, which is most likely a consequence of the missing correction for spin−orbit coupling, as such a DFT-based calculation is expected to underestimate the band gap.

Seebeck coefficient measurements of $Tl_{18}Pb_2Ti_7Se_{25}$ and $Tl_{18}Pb_2Zr_7Se_{25}$ confirm the semiconducting character with values above 100 μV K^{-1} (Figure 5). In particular the Zr-

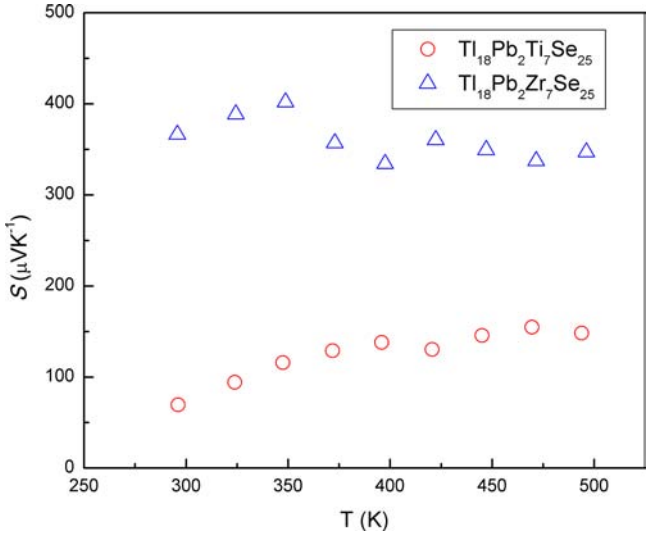

Figure 5. Seebeck coefficient of $Tl_{18}Pb_2Ti_7Se_{25}$ and $Tl_{18}Pb_2Zr_7Se_{25}$.

containing selenide with its S > 300 μV K^{-1} throughout the whole temperature range investigated has ample thermopower, so that increasing its carrier concentration via doping could easily still yield an acceptable Seebeck coefficient. The dominating carrier type of these undoped materials is p-type.

CONCLUSIONS

We have discovered an isostructural set of new quaternary chalcogenides, $Tl_{18}Pb_2M_7Q_{25}$, adopting a new structure type. The unit cell was identified to be cubic, space group $Pa\bar{3}$, with a large unit cell length of more than 17 Å for $Tl_{18}Pb_2Ti_7S_{25}$. The irregularities of the Tl coordination polyhedra due to the lone pair effect and weak Tl−Tl bonding cause the structure to be inherently complex. Interesting substructures are STl_6 octahedra, $[M_7Q_{24}]^{20-}$ finite, isolated anionic units, and supertetrahedral Tl_9Pb clusters.

We have calculated the electronic structure of representative compounds of this class as well as measured the electrical conductivity at and/or below room temperature. All of these compounds exhibit semiconducting behavior, with band gaps tunable between 0.10 to 1.0 eV by changing the metal and/or chalcogen atoms: all selenides and the Ti sulfide exhibit gaps below 0.5 eV, in part confirmed by an optical band gap measurement, and may thus be of interest for thermoelectric energy conversion, in combination with their complex crystal structure of high symmetry, the high content of heavy elements, and the large (positive) Seebeck coefficient of the undoped materials. Thus, we will commence to attempt to increase the charge carrier concentration of these intrinsic narrow-gap semiconductors via doping (e.g., by varying the Tl/Pb ratio), and then determine the thermoelectric properties of the doped samples after hot-pressing.

ASSOCIATED CONTENT

Supporting Information

Five crystallographic information files combined into one file (CIF), one DOS plot of $Tl_{18}Pb_2Ti_7Se_{25}$, and one diffuse

dx.doi.org/10.1021/ic3020699 | Inorg. Chem. 2013, 52, 1895−1900

reflectance spectrum of $Tl_{18}Pb_2Ti_7S_{25}$. This material is available free of charge via the Internet at http://pubs.acs.org.

AUTHOR INFORMATION

Corresponding Author

*E-mail: kleinke@uwaterloo.ca.

Notes

The authors declare no competing financial interest.

ACKNOWLEDGMENTS

Financial support from the Natural Sciences and Engineering Research Council is appreciated.

REFERENCES

(1) Rowe, D. M. *Thermoelectrics Handbook: Macro to Nano*; CRC Press, Taylor & Francis Group: Boca Raton, FL, 2006.
(2) Snyder, G. J.; Toberer, E. S. *Nat. Mater.* **2008**, *7*, 105−114.
(3) Sootsman, J. R.; Chung, D. Y.; Kanatzidis, M. G. *Angew. Chem., Int. Ed.* **2009**, *48*, 8616−8639.
(4) Wölfing, B.; Kloc, C.; Teubner, J.; Bucher, E. *Phys. Rev. Lett.* **2001**, *86*, 4350−4353.
(5) Johnsen, S.; Liu, Z. F.; Peters, J. A.; Song, J. H.; Peter, S. C.; Malliakas, C. D.; Cho, N. K.; Jin, H. S.; Freeman, A. J.; Wessels, B. W.; Kanatzidis, M. G. *Chem. Mater.* **2011**, *23*, 3120−3128.
(6) Johnsen, S.; Peter, S. C.; Nguyen, S. L.; Song, J. H.; Jin, H.; Freeman, A. J.; Kanatzidis, M. G. *Chem. Mater.* **2011**, *23*, 4375−4383.
(7) Kahler, D.; Singh, N. B.; Knuteson, D. J.; Wagner, B.; Berghmans, A.; McLaughlin, S.; King, M.; Schwartz, K.; Suhre, D.; Gotlieb, M. *Nucl. Instrum. Meth. Phys. Res., Sect. A* **2011**, *652*, 183−185.
(8) Owens, A. *J. Synchrotron Radiat.* **2006**, *13*, 143−150.
(9) Kurosaki, K.; Uneda, H.; Muta, H.; Yamanaka, S. *J. Alloys Compd.* **2004**, *376*, 43−48.
(10) Kurosaki, K.; Kosuga, A.; Yamanaka, S. *J. Alloys Compd.* **2003**, *351*, 279−282.
(11) Sankar, C. R.; Bangarigadu-Sanasy, S.; Kleinke, H. *J. Elecron. Mater.* **2012**, *41*, 1662−1666.
(12) Skoug, E. J.; Morelli, D. T. *Phys. Rev. Lett.* **2011**, *107*, 235901.
(13) Sankar, C. R.; Kuropatwa, B. A.; Assoud, A.; Kleinke, H. *Dalton Trans.* **2012**, *41*, 9646.
(14) Sankar, C. R.; Guch, M.; Assoud, A.; Kleinke, H. *Chem. Mater.* **2011**, *23*, 3886−3891.
(15) Sankar, C. R.; Bangarigadu-Sanasy, S.; Assoud, A.; Kleinke, H. *Inorg. Chem.* **2011**, *50*, 245−249.
(16) Sankar, C. R.; Bangarigadu-Sanasy, S.; Assoud, A.; Kleinke, H. *J. Mater. Chem.* **2010**, *20*, 7485−7490.
(17) Klepp, K. O.; Kolb, A. *Z. Naturforsch. B* **1999**, *54*, 441−446.
(18) Harringer, N. A.; Kolb, A.; Klepp, K. O. *Z. Naturforsch. B* **2001**, *56*, 1322−1324.
(19) Keane, P. M.; Ibers, J. A. *J. Solid State Chem.* **1991**, *93*, 291−297.
(20) Mitchell, J. F.; Burdett, J. K.; Keane, P. M.; Ibers, J. A.; DeGroot, D. C.; Hogan, T. P.; Schindler, J. L.; Kannewurf, C. R. *J. Solid State Chem.* **1992**, *99*, 103−9.
(21) Klepp, K. O.; Gurtner, D. *J. Alloys Compd.* **1996**, *243*, 6−11.
(22) Eulenberger, G. *Z. Kristallogr.* **1977**, *145*, 427−436.
(23) Sabov, M. Y.; Sevryukov, D. V.; Galagovets, I. V.; Betsa, V. V.; Peresh, E. Y. *Inorg. Mater.* **2010**, *46*, 11−13.
(24) Klepp, K. O.; Eulenberger, G. *Z. Naturforsch. B* **1984**, *39*, 705−712.
(25) Eulenberger, G. *Monatsh. Chem.* **1982**, *113*, 859−867.
(26) Kosuga, A.; Kurosaki, K.; Muta, H.; Yamanaka, S. In *Materials and Technologies for Direct Thermal-to-Electric Energy Conversion*; Yang, J., Hogan, T. P., Funahashi, R., Nolas, G. S., Eds.; Materials Research Society: Warrendale, PA, 2006; Vol. *886*, pp 343−347.
(27) Kosuga, A.; Kurosaki, K.; Muta, H.; Yamanaka, S. *J. Appl. Phys.* **2006**, *99*, 063705.
(28) *SAINT*, 4th ed.; Siemens Analytical X-ray Instruments Inc.: Madison, WI, 1995.
(29) *APEX2, User Manual*; Bruker AXS Inc.: Madison, WI, 2006.
(30) Sheldrick, G. M. *Acta Crystallogr. A* **2008**, *64*, 112−122.
(31) Spek, A. L. *J. Appl. Crystallogr.* **2003**, *36*, 7−13.
(32) Blaha, P.; Schwarz, K.; Madsen, G. K. H.; Kvasnicka, D.; Luitz, J. *WIEN2k, An Augmented Plane Wave + Local Orbitals Program for Calculating Crystal Properties*, version 10.1; Technical Universität Wien: Vienna, Austria, 2001.
(33) Perdew, J. P.; Burke, K.; Ernzerhof, M. *Phys. Rev. Lett.* **1996**, *77*, 3865−3868.
(34) Perdew, J. P.; Burke, K.; Ernzerhof, M. *Phys. Rev. Lett.* **1997**, *78*, 1396−1396.
(35) Guch, M.; Sankar, C. R.; Salvador, J. R.; Meisner, G. P.; Kleinke, H. *J. Appl. Phys.* **2012**, *111*, 063706/1−063706/6.
(36) Bangarigadu-Sanasy, S.; Sankar, C. R.; Schlender, P.; Kleinke, H. *J. Alloys Compd.* **2013**, *594*, 126−134.
(37) McTaggart, F. K.; Wadsley, A. D. *Aust. J. Chem.* **1958**, *11*, 445−457.
(38) Assoud, A.; Soheilnia, N.; Kleinke, H. *Chem. Mater.* **2005**, *17*, 4509−4513.
(39) Zhang, X.; Schindler, J. L.; Hogan, T.; Albritton-Thomas, J.; Kannewurf, C. R.; Kanatzidis, M. G. *Angew. Chem., Int. Ed. Engl.* **1995**, *34*, 68−71.
(40) Giester, G.; Lengauer, C. L.; Tillmanns, E.; Zemann, J. *J. Solid State Chem.* **2002**, *168*, 322−330.
(41) Ravindra, N. M.; Srivastava, V. K. *Phys. Status Solidi A* **1980**, *58*, 311−316.
(42) Lelieveld, R.; Ijdo, D. J. W. *Acta Crystallogr., Sect. B* **1978**, *34*, 3348−3349.
(43) Brese, N. E.; O'Keeffe, M. *Acta Crystallogr., Sect. B* **1991**, *47*, 192−197.
(44) Schewe, I.; Böttcher, P.; von Schnering, H. G. *Z. Kristallogr.* **1989**, *188*, 287−298.
(45) Cerny, R.; Joubert, J. M.; Filinchuk, Y.; Feutelais, Y. *Acta Crystallogr., Sect. C: Cryst. Struct. Commun.* **2002**, *58*, i63−i65.
(46) Stöwe, K. *J. Solid State Chem.* **2000**, *149*, 123−132.
(47) Dehnen, S.; Melullis, M. *Coord. Chem. Rev.* **2007**, *251*, 1259−1280.
(48) Palchik, O.; Iyer, R. G.; Liao, J. H.; Kanatzidis, M. G. *Inorg. Chem.* **2003**, *42*, 5052−5054.
(49) Wu, T.; Zuo, F.; Wang, L.; Bu, X.; Zheng, S.-T.; Ma, R.; Feng, P. *J. Am. Chem. Soc.* **2011**, *133*, 15886−15889.
(50) Wu, T.; Bu, X.; Zhao, X.; Khazhakyan, R.; Feng, P. *J. Am. Chem. Soc.* **2011**, *133*, 9616−9625.
(51) Wu, T.; Bu, X.; Liao, P.; Wang, L.; Zheng, S.-T.; Ma, R.; Feng, P. *J. Am. Chem. Soc.* **2012**, *134*, 3619−3622.
(52) Cahill, C. L.; Parise, J. B. *Chem. Mater.* **1997**, *9*, 807−811.
(53) Yaghi, O. M.; Sun, Z.; Richardson, D. A.; Groy, T. L. *J. Am. Chem. Soc.* **1994**, *116*, 807−808.
(54) Dong, Z. C.; Corbett, J. D. *Inorg. Chem.* **1996**, *35*, 1444−1450.
(55) Garcia, E.; Corbett, J. D. *Inorg. Chem.* **1990**, *29*, 3274−3282.
(56) Corbett, J. D. *Inorg. Chem.* **2000**, *39*, 5178−5191.
(57) Dong, Z. C.; Corbett, J. D. *J. Am. Chem. Soc.* **1993**, *115*, 11299−11303.
(58) Li, B.; Corbett, J. D. *Inorg. Chem.* **2004**, *43*, 3582−3587.
(59) Karpov, A.; Jansen, M. *Angew. Chem., Int. Ed.* **2005**, *44*, 7639−7643.
(60) Karpov, A.; Jansen, M. *Chem. Commun.* **2006**, 1706−1708.
(61) Saltykov, V.; Nuss, J.; Wedig, U.; Jansen, M. *Z. Anorg. Allg. Chem.* **2011**, *637*, 357−361.
(62) Tao, X.; Jund, P.; Viennois, R.; Tédenac, J.-C. *J. Phys. Chem. A* **2011**, *115*, 8761−8766.
(63) Larson, P.; Mahanti, S. D.; Chung, D.-Y.; Kanatzidis, M. G. *Phys. Rev. B* **2002**, *65*, 045205/1−045205/5.
(64) Chung, D.-Y.; Hogan, T. P.; Rocci-Lane, M.; Brazis, P.; Ireland, J. R.; Kannewurf, C. R.; Bastea, M.; Uher, C.; Kanatzidis, M. G. *J. Am. Chem. Soc.* **2004**, *126*, 6414−6428.